ELSEVIER

Journal of Neuroscience Methods 150 (2006) 228–237

JOURNAL OF NEUROSCIENCE METHODS

www.elsevier.com/locate/jneumeth

Frequency decomposition of conditional Granger causality and application to multivariate neural field potential data

Yonghong Chen[a,*], Steven L. Bressler[b], Mingzhou Ding[a]

[a] *Department of Biomedical Engineering, University of Florida, 102B BME Building, Gainesville, FL 32611-6131, USA*
[b] *Center for Complex Systems and Brain Sciences, Florida Atlantic University, Boca Raton, FL 33431, USA*

Received 7 April 2005; received in revised form 17 June 2005; accepted 20 June 2005

Abstract

It is often useful in multivariate time series analysis to determine statistical causal relations between different time series. Granger causality is a fundamental measure for this purpose. Yet the traditional pairwise approach to Granger causality analysis may not clearly distinguish between direct causal influences from one time series to another and indirect ones acting through a third time series. In order to differentiate direct from indirect Granger causality, a conditional Granger causality measure in the frequency domain is derived based on a partition matrix technique. Simulations and an application to neural field potential time series are demonstrated to validate the method.

Keywords: Granger causality; Conditional Granger causality; Multiple time series; Frequency domain; Multivariate autoregressive (MVAR) model; Autoregressive moving average (ARMA) process; Partition matrix

1. Introduction

The concept of causality introduced by Wiener (1956) and formulated by Granger (1969) has played a considerable role in investigating the relations among stationary time series. The original definition of Granger (1969), which is well named as Granger causality, refers to the improvement in predictability of a series that derives from incorporation of the past of a second series, above the predictability based solely on the past of the first series. This definition only involves the relation between two time series. As pointed out by Granger (1969, 1980), if a third series is taken into account, a spurious or indirect causality due to the third series may be detected. Then he defined a prima facie cause (Granger, 1980): Y is said to be a prima facie cause of X if the observations of Y up to time t ($Y(\tau) : \tau \leq t$) help one predict $X(t+1)$ when the corresponding observations of X and Z are available ($X(\tau)$, $Z(\tau) : \tau \leq t$). We refer to this idea as conditional Granger causality since it gives a measure of causality between two time series, X and Y, conditional on a third, Z. Evaluation of this conditional Granger causality in the time domain is fairly straightforward through comparison of two predictions of $X(t+1)$, one when ($X(\tau)$, $Z(\tau) : \tau \leq t$) are given, the other when ($X(\tau)$, $Y(\tau)$, $Z(\tau) : \tau \leq t$) are given. However, evaluating causality by frequency decomposition may allow more meaningful interpretations in cases where oscillations are involved.

After giving clear measurements of linear dependence and feedback between two blocks of time series (Geweke, 1982), he also presented a measure of conditional linear dependence and feedback (Geweke, 1984) . Both a time domain measure, consistent with that of Granger, and its frequency decomposition were given. Although Hosoya presented some improvements on Geweke's methods (both bivariate (Hosoya, 1991) and conditional versions (Hosoya, 2001)), they have not been widely accepted because his time domain implementation departs from Granger's original idea, and its physical interpretation is less clear.

We point out that Geweke's use of the term "feedback" is equivalent to "causality" in the present discussion. In applying Geweke's frequency-domain conditional Granger causality measure to neural field potential data, we have found that

* Corresponding author. Tel.: +1 352 392 5605; fax: +1 352 392 9791.
E-mail addresses: ychen@bme.ufl.edu (Y. Chen); bressler@fau.edu (S.L. Bressler); mding@bme.ufl.edu (M. Ding).

0165-0270/$ – see front matter © 2005 Elsevier B.V. All rights reserved.
doi:10.1016/j.jneumeth.2005.06.011

negative values, which have no meaning in terms of causality, may occur at some frequencies. This finding casts doubt on the applicability of Geweke's method for neural time series analysis. We believe that the negative values result from the lack of identity of estimates of the same spectrum when different autoregressive (AR) models are used. This non-identity of different estimates of the same spectrum is a general practical problem in numerical analysis that causes errors in Geweke's implementation because it requires the estimates to be identical. In this paper, we employ a partition matrix method to overcome this problem. Comparison of the results from our procedure with Geweke's original procedure, clearly shows the validity of the current procedure. In the following sections: we first provide an introduction to Granger causality; then present an overview of Geweke's procedure on conditional causality, pointing out the importance of obtaining a correct measure; and then derive our procedure. Finally, results of simulations and application to neural field potential time series data are provided.

2. Background

Consider a multiple stationary time series of dimension n, $\mathbf{W} = \{\mathbf{w}_t\}$. The series has the following moving average representation with use of the lag operator L:

$$\mathbf{w}_t = \mathbf{A}(L)\boldsymbol{\varepsilon}_t, \tag{1}$$

where $E(\boldsymbol{\varepsilon}_t) = 0$, $\mathrm{var}(\boldsymbol{\varepsilon}_t) = \boldsymbol{\Sigma}$ and $\mathbf{A}_0 = \mathbf{I}_n$, the $n \times n$ identity matrix. Assume there exists the autoregressive representation:

$$\mathbf{B}(L)\mathbf{w}_t = \boldsymbol{\varepsilon}_t, \tag{2}$$

where $\mathbf{B}_0 = \mathbf{I}_n$.

Suppose that $\mathbf{w}_t$ has been decomposed into two vectors $\mathbf{x}_t$ and $\mathbf{y}_t$ with k and l dimensions, respectively: $\mathbf{w}_t = (\mathbf{x}_t', \mathbf{y}_t')'$, where the prime denotes matrix transposition. Denote $\mathbf{W}_{t-1}$ as the subspace generated by $\{\mathbf{w}_s; s \le t-1\}$. Define $\boldsymbol{\Sigma}_1 = \mathrm{var}(\mathbf{x}_t|\mathbf{X}_{t-1})$, $\boldsymbol{\Sigma}_2 = \mathrm{var}(\mathbf{x}_t|\mathbf{X}_{t-1}, \mathbf{Y}_{t-1})$, $\mathbf{T}_1 = \mathrm{var}(\mathbf{y}_t|\mathbf{Y}_{t-1})$, $\mathbf{T}_2 = \mathrm{var}(\mathbf{y}_t|\mathbf{X}_{t-1}, \mathbf{Y}_{t-1})$ and $\boldsymbol{\Upsilon} = \mathrm{var}(\mathbf{w}_t|\mathbf{W}_{t-1})$, where the conditional variance is taken to be the variance of the residual about the linear projection which accounts for the prediction. The measures of linear causality from $\mathbf{Y}$ to $\mathbf{X}$, linear causality from $\mathbf{X}$ to $\mathbf{Y}$, instantaneous linear causality and linear dependence were respectively defined to be (Geweke, 1982):

$$\begin{aligned} F_{\mathbf{Y}\to\mathbf{X}} &= \ln(|\boldsymbol{\Sigma}_1|/|\boldsymbol{\Sigma}_2|), \\ F_{\mathbf{X}\to\mathbf{Y}} &= \ln(|\mathbf{T}_1|/|\mathbf{T}_2|), \\ F_{\mathbf{X}\cdot\mathbf{Y}} &= \ln(|\boldsymbol{\Sigma}_2| \cdot |\mathbf{T}_2|/|\boldsymbol{\Upsilon}|), \\ F_{\mathbf{X},\mathbf{Y}} &= \ln(|\boldsymbol{\Sigma}_1| \cdot |\mathbf{T}_1|/|\boldsymbol{\Upsilon}|) = F_{\mathbf{Y}\to\mathbf{X}} + F_{\mathbf{X}\to\mathbf{Y}} + F_{\mathbf{X}\cdot\mathbf{Y}}. \end{aligned} \tag{3}$$

The measures of directional linear causality may be decomposed by frequency. Let the autoregressive representation for $\mathbf{X}$ and $\mathbf{Y}$ be:

$$\begin{pmatrix} \mathbf{B}_{11}(L) & \mathbf{B}_{12}(L) \\ \mathbf{B}_{21}(L) & \mathbf{B}_{22}(L) \end{pmatrix} \begin{pmatrix} \mathbf{x}_t \\ \mathbf{y}_t \end{pmatrix} = \begin{pmatrix} \boldsymbol{\varepsilon}_{1t} \\ \boldsymbol{\varepsilon}_{2t} \end{pmatrix}, \tag{4}$$

with $\mathbf{B}_{11}(0) = \mathbf{I}_k$, $\mathbf{B}_{22}(0) = \mathbf{I}_l$, $\mathbf{B}_{12}(0) = 0$, $\mathbf{B}_{21}(0) = 0$, $\mathrm{var}(\boldsymbol{\varepsilon}_{1t}) = \boldsymbol{\Sigma}_2$, $\mathrm{var}(\boldsymbol{\varepsilon}_{2t}) = \mathbf{T}_2$. Eq. (4) is actually a partition form of Eq. (2). Let $\mathbf{C} = \mathrm{cov}(\boldsymbol{\varepsilon}_{1t}, \boldsymbol{\varepsilon}_{2t})$. Then pre-multiplying a transformation matrix

$$\mathbf{P} = \begin{pmatrix} \mathbf{I}_k & 0 \\ -\mathbf{C}'\boldsymbol{\Sigma}_2^{-1} & \mathbf{I}_l \end{pmatrix} \tag{5}$$

to both sides of Eq. (4), we have the following normalized form:

$$\begin{pmatrix} \tilde{\mathbf{B}}_{11}(L) & \tilde{\mathbf{B}}_{12}(L) \\ \tilde{\mathbf{B}}_{21}(L) & \tilde{\mathbf{B}}_{22}(L) \end{pmatrix} \begin{pmatrix} \mathbf{x}_t \\ \mathbf{y}_t \end{pmatrix} = \begin{pmatrix} \boldsymbol{\varepsilon}_{1t} \\ \tilde{\boldsymbol{\varepsilon}}_{2t} \end{pmatrix}, \tag{6}$$

where $\boldsymbol{\varepsilon}_{1t}$ and $\tilde{\boldsymbol{\varepsilon}}_{2t}$ are uncorrelated, $\mathrm{var}(\tilde{\boldsymbol{\varepsilon}}_{2t}) = \mathbf{T}_3 = \mathbf{T}_2 - \mathbf{C}'\boldsymbol{\Sigma}_2^{-1}\mathbf{C}$, and $\tilde{\mathbf{B}}_{12}(0) = 0$ but $\tilde{\mathbf{B}}_{21}(0) \neq 0$ in general. Then Eq. (6) implies the following spectral decomposition of the spectral density of X:

$$\mathbf{S}_{\mathbf{x}}(\lambda) = \tilde{\mathbf{H}}_{11}(\lambda)\boldsymbol{\Sigma}_2\tilde{\mathbf{H}}_{11}^*(\lambda) + \tilde{\mathbf{H}}_{12}(\lambda)\mathbf{T}_3\tilde{\mathbf{H}}_{12}^*(\lambda), \tag{7}$$

where $\tilde{\mathbf{H}}(\lambda)$ is the transfer matrix of the normalized autoregressive expression in Eq. (6). It is obvious that the spectral density of $\mathbf{X}$ is decomposed into an intrinsic part and a causal part, so the measure of linear causality was suggested as (Geweke, 1982):

$$f_{\mathbf{Y}\to\mathbf{X}}(\lambda) = \ln \frac{|\mathbf{S}_{\mathbf{x}}(\lambda)|}{|\tilde{\mathbf{H}}_{11}(\lambda)\boldsymbol{\Sigma}_2\tilde{\mathbf{H}}_{11}^*(\lambda)|}. \tag{8}$$

There is also a convergence relation between the measures in the time and frequency domains:

$$\frac{1}{2\pi}\int_{-\pi}^{\pi} f_{\mathbf{Y}\to\mathbf{X}}(\lambda)\,\mathrm{d}\lambda \le F_{\mathbf{Y}\to\mathbf{X}}. \tag{9}$$

In the above, a Granger causality measure between two (or two blocks of) time series was given. Before Geweke presented his logarithm version, Pierce (1979) had introduced a R^2 measure which simply takes the ratio of the variances of two prediction errors. The value of Pierce's R^2 measure is within [0, 1] which is more convenient for comparison with correlation coefficients. However, Geweke's logarithm version has better statistical properties. There has also been a measure based on autoregressive moving average (ARMA) models (Boudjellaba et al., 1992).

Granger causality analysis has been employed in a number of studies of neural data (Bernasconi and König, 1999; Bernasconi et al., 2000; Kaminski et al., 2001; Hesse et al., 2003; Harrison et al., 2003; Brovelli et al., 2004; Roebroek et al., 2005). The procedure described above has potential applications in these types of study. For those cases where more than two scalar/block time series recordings are available, the procedure may be performed to identify further patterns

of neural interaction after a more traditional pairwise analysis. We now consider two simple simulations to illustrate situations in which conditional Granger causality analysis is important.

2.1. Example 1: the case of differentially delayed driving

We first consider a simple system consisting of three variables, each representing an AR process:

$$\begin{aligned} x(t) &= \xi(t) \\ y(t) &= x(t-1) + \eta(t) \\ z(t) &= \mu z(t-1) + x(t-2) + \epsilon(t). \end{aligned} \tag{10}$$

where $|\mu| < 1$ is a parameter, and $\xi(t), \eta(t), \epsilon(t)$ are independent white noise processes with zero mean and variances $\sigma_1^2, \sigma_2^2, \sigma_3^2$, respectively. The system configuration is illustrated in Fig. 1(a) where x drives y after the delay of one time unit and x drives z after the delay of two time units. We note that the time unit here is arbitrary and has no physical meaning. To be consistent with the data presented later we assume that the sample rate is 200 Hz. In other words each time unit is 5 ms.

We performed a simulation of this system, with $\mu = 0.5, \sigma_1 = 1, \sigma_2 = 0.2$, and $\sigma_3 = 0.3$, to generate a data set of 500 realizations, each 100 points long. Then, assuming no knowledge of Eq. (10), we fit multivariate autoregressive (MVAR) models (Ding et al., 2000) to the generated data set for each pairwise combination of variables x, y, and z, and calculated the frequency-domain Granger causality for each pair in each direction, as shown in Fig. 1(b). In the top two rows of this figure, we see non-zero Granger causality values across the spectra of $\mathbf{x} \to \mathbf{y}$ and $\mathbf{x} \to \mathbf{z}$ and zero values across the spectra of $\mathbf{y} \to \mathbf{x}$ and $\mathbf{z} \to \mathbf{x}$. These results are indicative of the true unidirectional causal driving of y and z by x. However, we also see results in the third row of Fig. 1(b) which appear to indicate unidirectional causal driving of z by y. In fact, we know from the system configuration that this apparent driving is due to the common influence of x on both y and z but with different time delays. This mistaken identification of an indirect influence as being a direct one suggests the need for the conditional Granger causality measure.

2.2. Example 2: the case of sequential driving

Next we consider another simple system, again consisting of three AR processes:

$$\begin{aligned} x(t) &= \xi(t) \\ y(t) &= x(t-1) + \eta(t) \\ z(t) &= \mu z(t-1) + y(t-1) + \epsilon(t). \end{aligned} \tag{11}$$

This system configuration consists of sequential driving from x to y, then from y to z as illustrated in Fig. 2(a). The same numbers of realizations and data points were generated for the same parameter values, and MVAR models were again fit to the data. The results of Granger causality analysis in Fig. 2(b) show an apparent unidirectional causal driving of z by x that is in fact due to the indirect influence through y. Again, the mistaken identification of an indirect influence as being direct suggests the need for the conditional Granger causality measure.

Note that, although the systems in the above two examples are very different, the results of pairwise Granger causality analysis seen in Figs. 1(b) and 2(b) are essentially the same, indicating that the analysis could not distinguish between the two systems. These two examples, although simple, thus plainly demonstrate that the pairwise measure of Granger causality by itself may be insufficient to reveal true system relations. We now describe the conditional Granger causality as a potentially useful tool for disambiguating such situations.

3. Geweke's measure of conditional feedback causality

Now suppose that $\mathbf{w}_t$ has been decomposed into three vectors $\mathbf{x}_t$, $\mathbf{y}_t$ and $\mathbf{z}_t$ with k, l and m dimensions, respectively: $\mathbf{w}_t = (\mathbf{x}_t', \mathbf{y}_t', \mathbf{z}_t')'$. The measure given by Geweke for the linear dependence of $\mathbf{X}$ on $\mathbf{Y}$, conditional on $\mathbf{Z}$, in the time domain (Geweke, 1984) is:

$$F_{\mathbf{Y}\to\mathbf{X}|\mathbf{Z}} = \ln \frac{\mathrm{var}(\mathbf{x}_t|\mathbf{X}_{t-1}, \mathbf{Z}_{t-1})}{\mathrm{var}(\mathbf{x}_t|\mathbf{X}_{t-1}, \mathbf{Y}_{t-1}, \mathbf{Z}_{t-1})}, \tag{12}$$

which is consistent with Granger's definition of a prima facie cause (Granger, 1980).

Time series prediction is achieved by the fitting of MVAR models. In order to implement Eq. (12), two MVAR models are involved. One is the following two-variable MVAR model:

$$\begin{pmatrix} \mathbf{D}_{11}(L) & \mathbf{D}_{12}(L) \\ \mathbf{D}_{21}(L) & \mathbf{D}_{22}(L) \end{pmatrix} \begin{pmatrix} \mathbf{x}_t \\ \mathbf{z}_t \end{pmatrix} = \begin{pmatrix} \boldsymbol{\Theta}_t \\ \boldsymbol{\Psi}_t \end{pmatrix}, \tag{13}$$

with the normalization $\mathbf{D}_{11}(0) = \mathbf{I}$, $\mathbf{D}_{22}(0) = \mathbf{I}$, $\mathbf{D}_{12}(0) = 0$, and $\mathrm{cov}(\boldsymbol{\Theta}_t, \boldsymbol{\Psi}_t) = 0$ imposed in order to yield the frequency decomposition of the conditional dependence. The normalization can be achieved by using a transformation matrix like Eq. (5).

The other MVAR model used for deriving the frequency decomposition of the conditional dependence is the following three-variable MVAR model:

$$\begin{pmatrix} \mathbf{B}_{11}(L) & \mathbf{B}_{12}(L) & \mathbf{B}_{13}(L) \\ \mathbf{B}_{21}(L) & \mathbf{B}_{22}(L) & \mathbf{B}_{23}(L) \\ \mathbf{B}_{31}(L) & \mathbf{B}_{32}(L) & \mathbf{B}_{33}(L) \end{pmatrix} \begin{pmatrix} \mathbf{x}_t \\ \mathbf{y}_t \\ \mathbf{z}_t \end{pmatrix} = \begin{pmatrix} \boldsymbol{\varepsilon}_{xt} \\ \boldsymbol{\varepsilon}_{yt} \\ \boldsymbol{\varepsilon}_{zt} \end{pmatrix}, \tag{14}$$

with normalization imposed too. The explicit formula of the transformation matrix to normalize the MVAR model of three time series is given in the Appendix A.

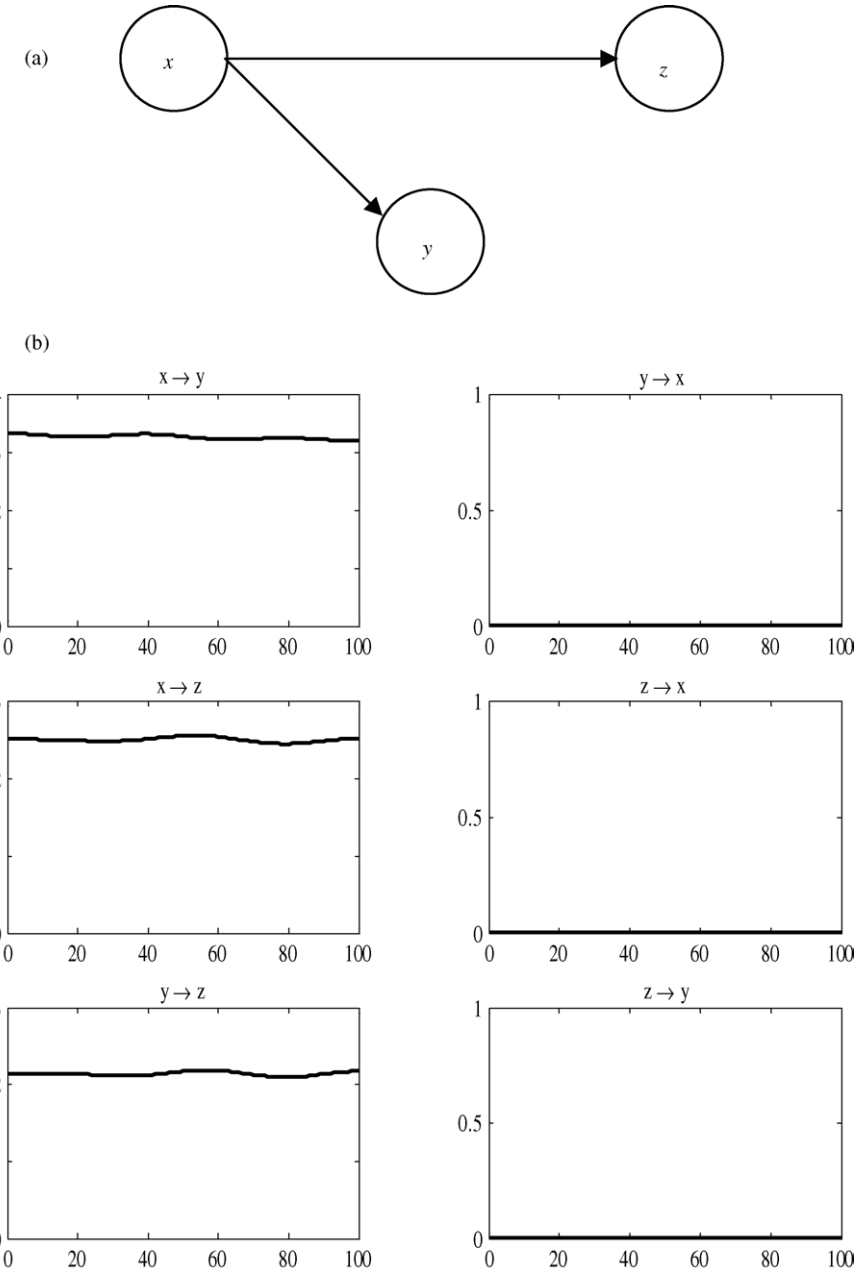

Fig. 1. (a) Schematic illustration of a simple delay driving system; (b) Granger causality spectra by pairwise analysis.

Based on the relations of different variances, Geweke derived the following important relation of the conditional causality in the time domain (Geweke, 1984):

$$F_{\mathbf{Y}\to\mathbf{X}|\mathbf{Z}} = F_{\mathbf{Y}\boldsymbol{\Psi}\to\boldsymbol{\Theta}}. \tag{15}$$

The same relationship is satisfied in the frequency domain (Geweke, 1984):

$$f_{\mathbf{Y}\to\mathbf{X}|\mathbf{Z}}(\lambda) = f_{\mathbf{Y}\boldsymbol{\Psi}\to\boldsymbol{\Theta}}(\lambda). \tag{16}$$

In order to get $f_{\mathbf{Y}\boldsymbol{\Psi}\to\boldsymbol{\Theta}}(\lambda)$, we need to decompose the variance of $\boldsymbol{\Theta}$ into the frequency domain. To do so, we write Eqs. (13) and (14) in the frequency domain:

$$\begin{pmatrix}\mathbf{X}(\lambda)\\ \mathbf{Z}(\lambda)\end{pmatrix} = \begin{pmatrix}\mathbf{G}_{xx}(\lambda) & \mathbf{G}_{xz}(\lambda)\\ \mathbf{G}_{zx}(\lambda) & \mathbf{G}_{zz}(\lambda)\end{pmatrix}\begin{pmatrix}\boldsymbol{\Theta}(\lambda)\\ \boldsymbol{\Psi}(\lambda)\end{pmatrix}, \tag{17}$$

$$\begin{pmatrix}\mathbf{X}(\lambda)\\ \mathbf{Y}(\lambda)\\ \mathbf{Z}(\lambda)\end{pmatrix} = \begin{pmatrix}\mathbf{H}_{xx}(\lambda) & \mathbf{H}_{xy}(\lambda) & \mathbf{H}_{xz}(\lambda)\\ \mathbf{H}_{yx}(\lambda) & \mathbf{H}_{yy}(\lambda) & \mathbf{H}_{yz}(\lambda)\\ \mathbf{H}_{zx}(\lambda) & \mathbf{H}_{zy}(\lambda) & \mathbf{H}_{zz}(\lambda)\end{pmatrix}\begin{pmatrix}\mathbf{E}_x(\lambda)\\ \mathbf{E}_y(\lambda)\\ \mathbf{E}_z(\lambda)\end{pmatrix}. \tag{18}$$

If the spectra of $\mathbf{X}(\lambda)$ and $\mathbf{Z}(\lambda)$ from Eq.(17) remain identical to the spectra from Eq. (18), then we can substitute Eq. (17)

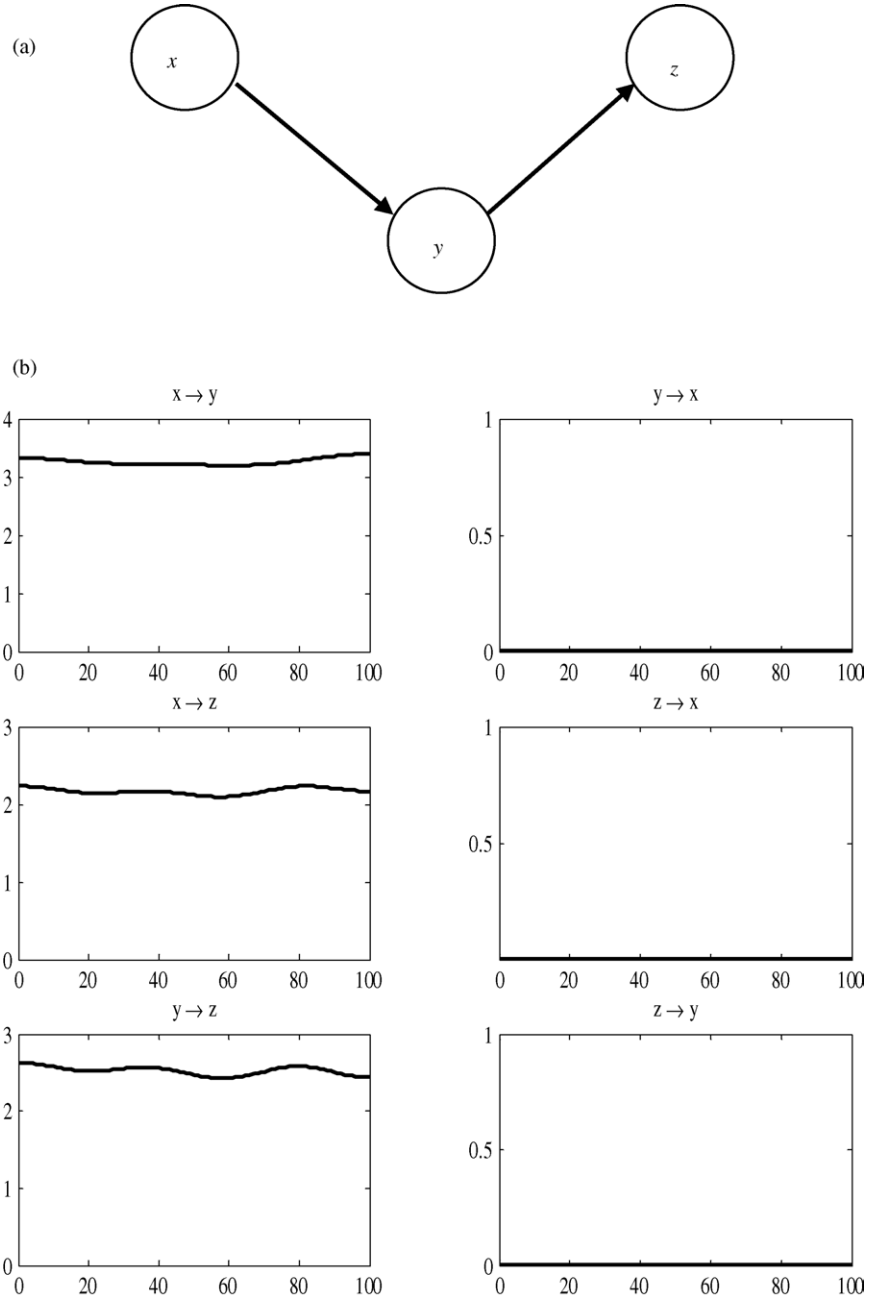

Fig. 2. (a) Schematic illustration of a simple sequential driving system; (b) Granger causality spectra by pairwise analysis.

into Eq. (18) to get the following equations:

$$\begin{pmatrix} \boldsymbol{\Theta}(\lambda) \\ \mathbf{Y}(\lambda) \\ \boldsymbol{\Psi}(\lambda) \end{pmatrix} = \begin{pmatrix} \mathbf{G}_{xx}(\lambda) & 0 & \mathbf{G}_{xz}(\lambda) \\ 0 & \mathbf{I}_l & 0 \\ \mathbf{G}_{zx}(\lambda) & 0 & \mathbf{G}_{zz}(\lambda) \end{pmatrix}^{-1} \begin{pmatrix} \mathbf{H}_{xx}(\lambda) & \mathbf{H}_{xy}(\lambda) & \mathbf{H}_{xz}(\lambda) \\ \mathbf{H}_{yx}(\lambda) & \mathbf{H}_{yy}(\lambda) & \mathbf{H}_{yz}(\lambda) \\ \mathbf{H}_{zx}(\lambda) & \mathbf{H}_{zy}(\lambda) & \mathbf{H}_{zz}(\lambda) \end{pmatrix} \begin{pmatrix} \mathbf{E}_x(\lambda) \\ \mathbf{E}_y(\lambda) \\ \mathbf{E}_z(\lambda) \end{pmatrix}$$

$$= \begin{pmatrix} \mathbf{Q}_{xx}(\lambda) & \mathbf{Q}_{xy}(\lambda) & \mathbf{Q}_{xz}(\lambda) \\ \mathbf{Q}_{yx}(\lambda) & \mathbf{Q}_{yy}(\lambda) & \mathbf{Q}_{yz}(\lambda) \\ \mathbf{Q}_{zx}(\lambda) & \mathbf{Q}_{zy}(\lambda) & \mathbf{Q}_{zz}(\lambda) \end{pmatrix} \begin{pmatrix} \mathbf{E}_x(\lambda) \\ \mathbf{E}_y(\lambda) \\ \mathbf{E}_z(\lambda) \end{pmatrix}, \tag{19}$$

where $\mathbf{Q}(\lambda) = \mathbf{G}^{-1}(\lambda)\mathbf{H}(\lambda)$. From the first equation of Eq. (19), the spectrum of $\boldsymbol{\Theta}$ is decomposed into the following

three obvious parts:

$$\mathbf{S}_\Theta(\lambda) = \mathbf{Q}_{xx}(\lambda)\boldsymbol{\Sigma}_{xx}\mathbf{Q}^*_{xx}(\lambda) + \mathbf{Q}_{xy}(\lambda)\boldsymbol{\Sigma}_{yy}\mathbf{Q}^*_{xy}(\lambda) + \mathbf{Q}_{xz}(\lambda)\boldsymbol{\Sigma}_{zz}\mathbf{Q}^*_{xz}(\lambda). \quad (20)$$

Therefore, the measure of causality from $\mathbf{Y}\boldsymbol{\Psi}$ to $\boldsymbol{\Theta}$ may be described as:

$$f_{\mathbf{Y}\boldsymbol{\Psi}\to\boldsymbol{\Theta}}(\lambda) = \ln \frac{|\mathbf{S}_\Theta(\lambda)|}{|\mathbf{Q}_{xx}(\lambda)\boldsymbol{\Sigma}_{xx}\mathbf{Q}^*_{xx}(\lambda)|}, \quad (21)$$

where $\mathbf{S}_\Theta(\lambda)$ is actually the variance of $\boldsymbol{\Theta}_t$, namely $\boldsymbol{\Sigma}_\Theta$, since $\boldsymbol{\Theta}_t$ is white noise in Eq. (13). Considering the relation of Eq. (16), we could get the conditional causality as Geweke (1984):

$$f_{\mathbf{Y}\to\mathbf{X}|\mathbf{Z}}(\lambda) = \ln \frac{|\boldsymbol{\Sigma}_\Theta|}{|\mathbf{Q}_{xx}(\lambda)\boldsymbol{\Sigma}_{xx}\mathbf{Q}^*_{xx}(\lambda)|}, \quad (22)$$

In the above derivations, the assumption that the spectra of $\mathbf{X}(\lambda)$ and $\mathbf{Z}(\lambda)$ coming from Eq. (17) and from Eq.(18) are identical is actually very hard to satisfy numerically due to practical estimation errors. As an example of this problem, consider Fig. 6, where the dashed curves result from performing Geweke's conditional causality procedure. Note that the negative values seen here have no interpretation in terms of causality. (A detailed description of Fig. 6 is given in a later section.) In the following section, we introduce the partition matrix technique to overcome this problem.

4. Partition matrix improvement

For three blocks of time series $\mathbf{x}_t$, $\mathbf{y}_t$, $\mathbf{z}_t$, we can fit a three-variable MVAR model as in Eq.(14) and we can also derive its frequency domain expression as in Eq. (18). From Eq. (18), writing an expression only for $\mathbf{X}(\lambda)$ and $\mathbf{Z}(\lambda)$ (making partitions) we have:

$$\begin{pmatrix}\mathbf{X}(\lambda)\\ \mathbf{Z}(\lambda)\end{pmatrix} = \begin{pmatrix}\mathbf{H}_{xx}(\lambda) & \mathbf{H}_{xz}(\lambda)\\ \mathbf{H}_{zx}(\lambda) & \mathbf{H}_{zz}(\lambda)\end{pmatrix}\begin{pmatrix}\bar{\mathbf{E}}_x(\lambda)\\ \bar{\mathbf{E}}_z(\lambda)\end{pmatrix}, \quad (23)$$

where $\bar{\mathbf{E}}_x(\lambda)$ and $\bar{\mathbf{E}}_z(\lambda)$ have the following moving average expression:

$$\begin{pmatrix}\bar{\mathbf{E}}_x(\lambda)\\ \bar{\mathbf{E}}_z(\lambda)\end{pmatrix} = \begin{pmatrix}\mathbf{E}_x(\lambda)\\ \mathbf{E}_z(\lambda)\end{pmatrix} + \begin{pmatrix}\mathbf{H}_{xx}(\lambda) & \mathbf{H}_{xz}(\lambda)\\ \mathbf{H}_{zx}(\lambda) & \mathbf{H}_{zz}(\lambda)\end{pmatrix}^{-1} \times \begin{pmatrix}\mathbf{H}_{xy}(\lambda)\\ \mathbf{H}_{zy}(\lambda)\end{pmatrix}\mathbf{E}_y(\lambda). \quad (24)$$

We realize that Eq. (23) is actually a summation of multiple ARMA processes, and that the summation of several ARMA processes is still an ARMA process (Granger and Morris, 1976; Harvey, 1993). However, an unambiguous representation of the general multivariate ARMA process for the summation is unknown, although a general univariate ARMA model could be obtained through a specific procedure (Maravall and Mathis, 1994). Alternatively, we adopt the following procedure to evaluate the conditional Granger causality.

Letting

$$\begin{pmatrix}\bar{\mathbf{H}}_{xy}(\lambda)\\ \bar{\mathbf{H}}_{zy}(\lambda)\end{pmatrix} = \begin{pmatrix}\mathbf{H}_{xx}(\lambda) & \mathbf{H}_{xz}(\lambda)\\ \mathbf{H}_{zx}(\lambda) & \mathbf{H}_{zz}(\lambda)\end{pmatrix}^{-1}\begin{pmatrix}\mathbf{H}_{xy}(\lambda)\\ \mathbf{H}_{zy}(\lambda)\end{pmatrix},$$

we get the covariance matrix of the noise terms given in Eq. (24):

$$\bar{\boldsymbol{\Sigma}}(\lambda) = \begin{pmatrix}\boldsymbol{\Sigma}_{xx} & \boldsymbol{\Sigma}_{xz}\\ \boldsymbol{\Sigma}_{zx} & \boldsymbol{\Sigma}_{zz}\end{pmatrix} + \begin{pmatrix}\bar{\mathbf{H}}_{xy}(\lambda)\\ \bar{\mathbf{H}}_{zy}(\lambda)\end{pmatrix}(\boldsymbol{\Sigma}_{xy}\ \boldsymbol{\Sigma}_{zy}) + \begin{pmatrix}\boldsymbol{\Sigma}_{xy}\\ \boldsymbol{\Sigma}_{zy}\end{pmatrix}(\bar{\mathbf{H}}^*_{xy}(\lambda)\ \bar{\mathbf{H}}^*_{zy}(\lambda)) + \boldsymbol{\Sigma}_{yy}\begin{pmatrix}\bar{\mathbf{H}}_{xy}(\lambda)\\ \bar{\mathbf{H}}_{zy}(\lambda)\end{pmatrix}(\bar{\mathbf{H}}^*_{xy}(\lambda)\bar{\mathbf{H}}^*_{zy}(\lambda)). \quad (25)$$

This covariance matrix is no longer a real matrix, but it is a Hermite matrix, i.e. $\bar{\boldsymbol{\Sigma}}_{xz}(\lambda) = \bar{\boldsymbol{\Sigma}}^*_{zx}(\lambda)$. Therefore, we can use the following transformation matrix to normalize the bivariate model of Eq. (23):

$$\bar{\mathbf{P}} = \begin{pmatrix}\mathbf{I}_k & 0\\ -\dfrac{\bar{\boldsymbol{\Sigma}}_{xz}(\lambda)}{\boldsymbol{\Sigma}_{xx}} & \mathbf{I}_m\end{pmatrix}. \quad (26)$$

Therefore, in correspondence with the normalized form in Eq. (17), the transfer matrix $\mathbf{G}(\lambda)$ is now:

$$\mathbf{G}(\lambda) = \begin{pmatrix}\mathbf{H}_{xx}(\lambda) & \mathbf{H}_{xz}(\lambda)\\ \mathbf{H}_{zx}(\lambda) & \mathbf{H}_{zz}(\lambda)\end{pmatrix}\begin{pmatrix}\mathbf{I}_k & 0\\ -\dfrac{\bar{\boldsymbol{\Sigma}}_{xz}(\lambda)}{\boldsymbol{\Sigma}_{xx}} & \mathbf{I}_m\end{pmatrix}^{-1} \quad (27)$$

Taking the expansion form of this $\mathbf{G}(\lambda)$ matrix to get matrix $\mathbf{Q}(\lambda) = \mathbf{G}^{-1}(\lambda)\mathbf{H}(\lambda)$, and considering $\boldsymbol{\Sigma}_\Theta = \bar{\boldsymbol{\Sigma}}_{xx}$, where $\bar{\boldsymbol{\Sigma}}_{xx}$ comes from Eq. (25), we can still use Eq. (22) to get the conditional causality.

5. Applications to simulated and neural field potential data

5.1. Application to simulated data

We performed conditional Granger causality analysis on the delay driving and sequential driving systems presented above in Section 2. For the delay driving case (Section 2.1 and Fig. 1), the Granger causality spectrum from y to z, conditional on x, is presented in Fig. 3. It is obvious from Fig. 3 that the conditional Granger causality measure eliminated the indirect causal influence of y on z which appeared in Fig. 1(b). For the sequential driving case (Section 2.2 and Fig. 2), the Granger causality from x to z, conditional on y, is also

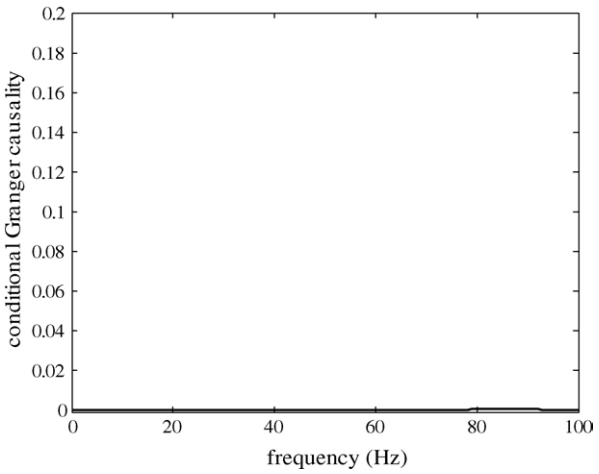

Fig. 3. Conditional Granger causality spectra from y to z, conditional on x, in the delay driving example (Fig. 1), and from x to z, conditional on y, in the sequential driving example (Fig. 2), showing that the indirect effects indicated in Figs. 1(b) and 2(b) have been eliminated.

presented in Fig. 3. Clearly, the indirect causal influence from x to z, which was indicated in Fig. 2(b), was also eliminated by use of the conditional Granger causality.

In both cases, we have seen that conditional Granger causality analysis eliminated indirect causal influences that inadvertently resulted from application of the pairwise Granger causality measure. Knowing the system equations in these examples allowed us to verify that the conditional Granger causality measure yielded a truer depiction of the system relations. We now consider how the conditional Granger causality measure may provide the same benefit in the analysis of real neural data.

5.2. Application to neural field potential data

Field potential data were recorded from two macaque monkeys using transcortical bipolar electrodes at 15 distributed sites in multiple cortical areas of one hemisphere (right hemisphere in monkey GE and left hemisphere in monkey LU) while the monkeys performed a GO/NO-GO visual pattern discrimination task (Bressler et al., 1993). The presence of oscillatory field potential activity in the beta (14–30 Hz) frequency range was recently reported in the sensorimotor cortex of these monkeys during the prestimulus period (Brovelli et al., 2004). In that study, Granger causality analysis was performed for all pairwise combinations of sensorimotor cortical recording sites. In both monkeys, significant Granger causal influences were discovered from primary somatosensory cortex to both primary motor cortex and inferior posterior parietal cortex, with the latter area also exerting Granger causal influences on primary motor cortex.

In monkey GE, the possibility existed that the causal influence from the primary somatosensory (*Soma*) site to one of the inferior posterior parietal sites (in area 7a) was actually mediated by another inferior posterior parietal site (in area 7b) (Fig. 4(a)). We therefore used conditional Granger causality analysis to test the hypothesis that the *Soma* → 7*a* influence was mediated by the 7*b* site. In Fig. 4(b) is presented the pairwise Granger causality spectrum from the *Soma* site to the 7*a* site (*Soma* → 7*a*, light solid curve), showing significant causal influence in the beta frequency range. Superimposed in Fig. 4(b) is the conditional Granger causality spectrum for the same pair, but with the 7*b* site taken into account (*Soma* → 7*a*|7*b*, dark solid curve). The corresponding 99% significance thresholds are also presented (light and dark dashed lines which overlap each other). These significance thresholds were determined using a permutation procedure (Edgington, 1980) that involved creating 500 permutations of the field potential data set by random rearrangement of the trial order. Since the test was performed separately for each frequency, a correction was necessary for the multiple comparisons over the whole range of frequencies. The Bonferroni correction could not be employed because these multiple comparisons were not independent. An alternative strategy was employed following (Blair and Karniski, 1993). The Granger causality spectrum was computed for each permutation, and then the maximum causality value over the frequency range was identified. After 500 permutation steps, a distribution of maximum causality values was created. Choosing a p-value at $p = 0.01$ for this distribution gave the thresholds shown in Fig. 4(b), (c) and Fig. 5(b) in dashed lines.

We see from Fig. 4(b) that the conditional Granger causality is greatly reduced in the beta frequency range and no longer significant, meaning that the causal influence from the *Soma* site to the 7*a* site is most likely an indirect effect mediated by the 7*b* site. This conclusion is consistent with the known neuroanatomy of the sensorimotor cortex (Felleman and Essen, 1991) in which area 7a is connected with area 7b, but not directly with the primary somatosensory cortex.

From Fig. 4(a) we see that the possibility also existed that the causal influence from the *Soma* site to the primary motor (*Mot*) site in monkey GE was mediated by the 7*b* site. To test this possibility, the Granger causality spectrum from *Soma* to *Mot* (*Soma* → *Mot*, light solid curve in Fig. 4(c)) was compared with the conditional Granger causality spectrum with 7*b* taken into account (*Soma* → *Mot*|7*b*, dark solid curve in Fig. 4(c)). In contrast to Fig. 4(b), we see that the beta-frequency conditional Granger causality in Fig. 4(c) is only partially reduced, and remains well above the 99% significance level. In Fig. 5(a), we see that the same possibility existed in monkey LU of the *Soma* to *Mot* causal influence being mediated by 7*b*. However, just as in Fig. 4(c), we see in Fig. 5(b) that the beta-frequency conditional Granger causality for monkey LU is only partially reduced, and remains well above the 99% significance level.

The results from both monkeys thus indicate that the Granger causal influence from the primary somatosensory cortex to the primary motor cortex was not simply an indirect effect mediated by area 7b. However, we further found that area 7b did play a role in mediating the *Soma* to *Mot*

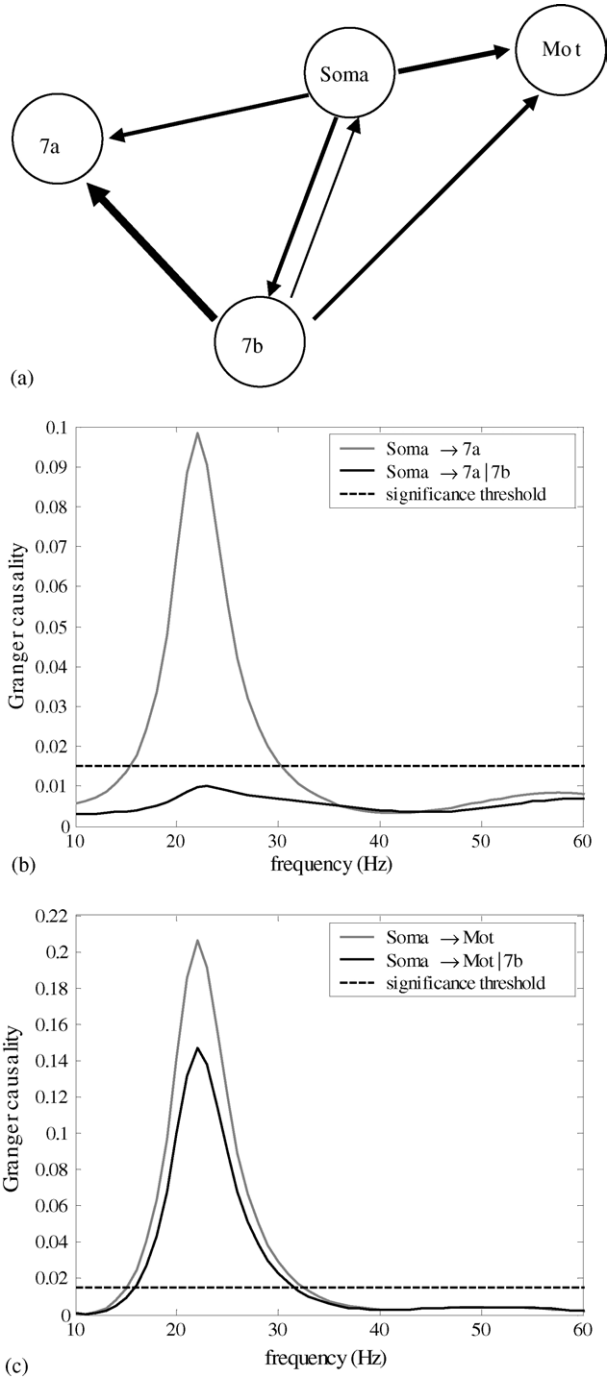

Fig. 4. Granger causality analysis of field potential data from monkey GE. (a) Schematic illustration of significant Granger causal influences in the beta frequency band among sites in sensorimotor cortex. (b) The reduction of the conditional Granger causality spectrum (dark solid line) below the significance threshold indicates an indirect influence of the primary somatosensory site on the 7*a* site. (c) The fact that the conditional Granger causality spectrum (dark solid line) does not fall below the significance threshold shows that there is a direct influence of the primary somatosensory site on the primary motor site. That the conditional spectrum is significantly below the pairwise spectrum indicates that there is an additional indirect effect mediated by 7b.

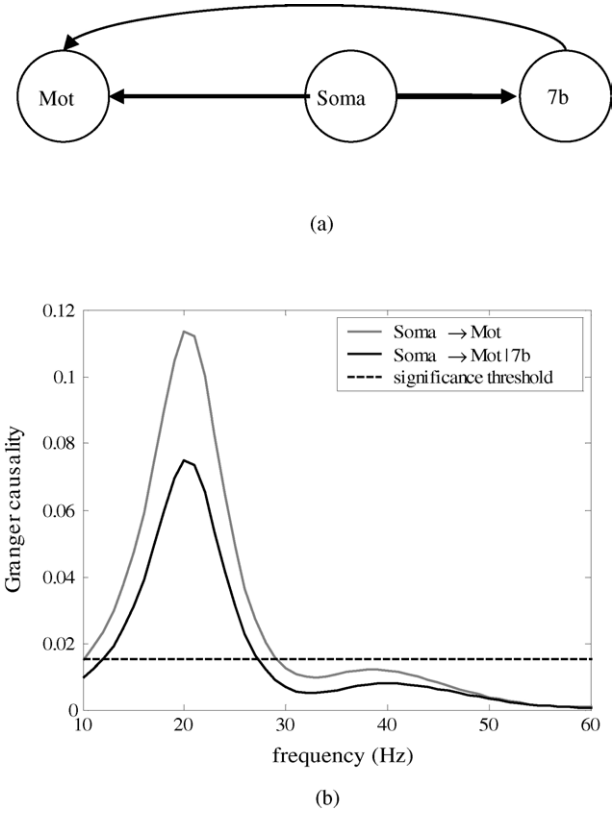

Fig. 5. Granger causality analysis of field potential data from monkey LU. (a) Schematic illustration of significant Granger causal influences in the beta frequency band among sites in sensorimotor cortex. (b) As in Fig. 4(c), the conditional Granger causality spectrum (dark solid line) does not fall below the significance threshold, indicating that there is a direct influence of the primary somatosensory site on the primary motor site. Again, the conditional spectrum is significantly below the pairwise spectrum, showing that there is an additional indirect effect mediated by 7b.

causal influence in both monkeys. This was determined by comparing the means of bootstrap resampled distributions of the peak beta Granger causality values from the spectra of $Soma \rightarrow Mot$ and $Soma \rightarrow Mot|7b$ by Student's t-test. The significant reduction of beta-frequency Granger causality when area 7b is taken into account ($t = 17.2$ for GE; $t = 18.2$ for LU, $p \lll 0.001$ for both), indicates that the influence from the primary somatosensory to primary motor area was partially mediated by area 7b. Such an influence is consistent with the known neuroanatomy (Felleman and Essen, 1991), which shows direct connections between area 7b and both primary motor and primary somatosensory areas.

As a final demonstration of the value of using the partition matrix method outlined in this paper to compute conditional Granger causality, we present in Fig. 6a direct comparison of our improved procedure (solid) with Geweke's original procedure (dashed) for the $Soma \rightarrow Mot|7b$ spectra of monkey GE (Fig. 6(a)) and monkey LU (Fig. 6(b)). From much previous experience working with this field potential data (Brovelli et al., 2004), we know that spec-

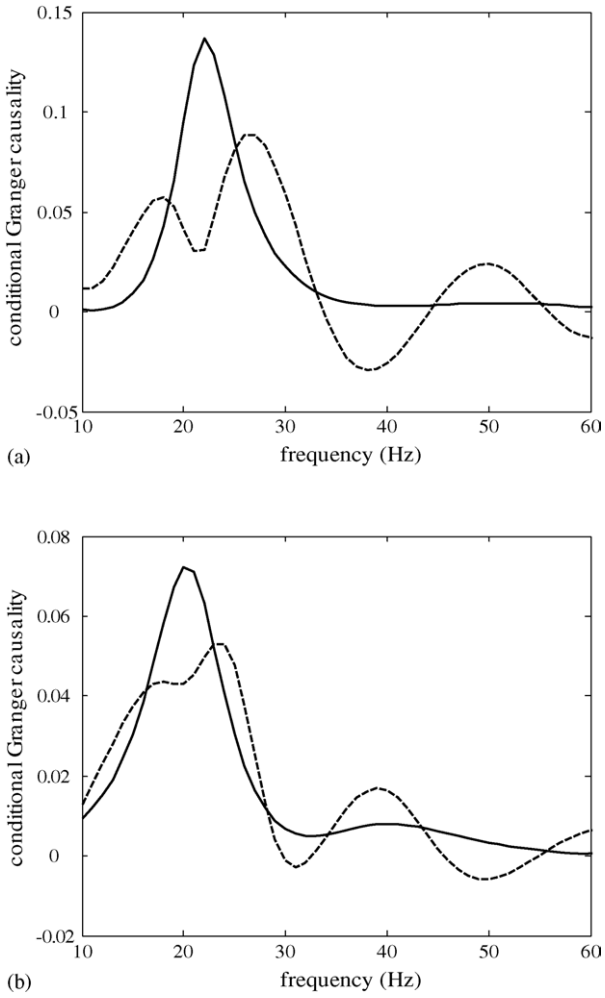

Fig. 6. Comparison of Geweke's original method for computing conditional Granger causality spectra (dashed) with our partition matrix procedure (solid). (a) *Soma* → *Mot*|*7b* in monkey GE, corresponding to Fig. 4(c); (b) *Soma* → *Mot*|*7b* in monkey LU, corresponding to Fig. 5(b). Note that for both monkeys, Geweke's original method suffers from having multiple peaks and valleys across the spectra (believed to be artifactual), and also from having negative values, which have no physical interpretation.

tra from these cortical areas typically have a single peak in the beta frequency range. Geweke's original method is clearly seen to be deficient in these examples not only by the multiple peaks and valleys across the spectra, but also by the negative values, which have no physical interpretation. We thus are confident that the partition matrix technique is a potentially valuable tool to be used in the investigation of conditional Granger causality relations between neural signals.

Acknowledgements

The work was supported by US NIMH grants MH64204, MH070498 and MH71620, and NSF grant 0090717.

Appendix A. Transformation matrix to normalize a model of three time series

Since the MVAR model, such as in Eq. (14), is usually not normalized, the noise terms could be correlated with each other. Let us assume that the covariance matrix is given by:

$$\mathbf{\Sigma} = \begin{pmatrix} \mathbf{\Sigma}_{xx} & \mathbf{\Sigma}_{xy} & \mathbf{\Sigma}_{xz} \\ \mathbf{\Sigma}_{yx} & \mathbf{\Sigma}_{yy} & \mathbf{\Sigma}_{yz} \\ \mathbf{\Sigma}_{zx} & \mathbf{\Sigma}_{zy} & \mathbf{\Sigma}_{zz} \end{pmatrix}.$$

In order to make the first noise term independent, we could use the following transform:

$$\mathbf{P}_1 = \begin{pmatrix} \mathbf{I}_k & 0 & 0 \\ -\mathbf{\Sigma}_{yx}\mathbf{\Sigma}_{xx}^{-1} & \mathbf{I}_l & 0 \\ -\mathbf{\Sigma}_{zx}\mathbf{\Sigma}_{xx}^{-1} & 0 & \mathbf{I}_m \end{pmatrix}.$$

Then the covariance matrix for the transformed noise terms is:

$$\begin{pmatrix} \mathbf{\Sigma}_{xx} & 0 & 0 \\ 0 & \mathbf{\Sigma}_{yy} - \mathbf{\Sigma}_{yx}\mathbf{\Sigma}_{xx}^{-1}\mathbf{\Sigma}_{xy} & \mathbf{\Sigma}_{yz} - \mathbf{\Sigma}_{yx}\mathbf{\Sigma}_{xx}^{-1}\mathbf{\Sigma}_{xz} \\ 0 & \mathbf{\Sigma}_{zy} - \mathbf{\Sigma}_{zx}\mathbf{\Sigma}_{xx}^{-1}\mathbf{\Sigma}_{xz} & \mathbf{\Sigma}_{zz} - \mathbf{\Sigma}_{zx}\mathbf{\Sigma}_{xx}^{-1}\mathbf{\Sigma}_{xz} \end{pmatrix}.$$

Again, to make the second and third noise terms independent, the following transformation may be made:

$$\mathbf{P}_2 = \begin{pmatrix} \mathbf{I}_k & 0 & 0 \\ 0 & \mathbf{I}_l & 0 \\ 0 & -(\mathbf{\Sigma}_{zy} - \mathbf{\Sigma}_{zx}\mathbf{\Sigma}_{xx}^{-1}\mathbf{\Sigma}_{xz})(\mathbf{\Sigma}_{yy} - \mathbf{\Sigma}_{yx}\mathbf{\Sigma}_{xx}^{-1}\mathbf{\Sigma}_{xy})^{-1} & \mathbf{I}_m \end{pmatrix}.$$

Therefore the whole transformation matrix needed to make all three noise terms independent is:

$$\mathbf{P} = \mathbf{P}_2 \cdot \mathbf{P}_1$$

References

Bernasconi C, König P. On the directionality of cortical interactions studied by structural analysis of electrophysiological recordings. Biol Cybern 1999;81:199–210.

Bernasconi C, von Stein A, Chiang C, König P. Bi-directional interactions between visual areas in the awake behaving cat. NeuroReport 2000;11;689–92.

Blair RC, Karniski W. An alternative method for significance testing of waveform differnce potentials. Psychophysiology 1993:30:518–24.

Boudjellaba H, Dufour J, Roy R. Testing causality between two vectors in multivariate autoregressive moving average models. J Am Stat Assoc 1992;87:1082–90.

Bressler SL, Coppola R, Nakamura R. Episodic multiregional cortical coherence at multiple frequencies during visual task performance. Nature 1993;366:153–6.

Brovelli A, Ding M, Ledberg A, Chen Y, Nakamura R, Bressler SL. Beta oscillatory in a large-scale sensorimotor cortical network: directional

influences revealed by Granger causality. Aroc Natl Acad Sci USA 2004;101:9849–54.
Ding M, Bressler SL, Yang W, Liang H. Short-window spectral analysis of cortical event-related potentials by adaptive multivariate autoregressive modeling: data preprocessing, model validation, and variability assessment. Biol Cybern 2000;83:35–45.
Edgington, ES. Randomization Tests. New York: Dekker; 1980.
Felleman DJ, Essen DCV. Distributed hierarchical processing in the cerebral cortex. Cerebral Cortex 1991;1:1–47.
Geweke J. Measurement of linear dependence and feedback between multiple time series. J Am Stat Assoc 1982;77:304–13.
Geweke J. Measures of conditional linear dependence and feedback between time series. J Am Stat Assoc 1984;79:907–15.
Granger CWJ. Investigating causal relations by econometric models and cross-spectral methods. Econometrica 1969;37:424–38.
Granger CWJ. Testing for causality: a personal viewpoint. J Econ Dynamics Control 1980;2:329–52.
Granger CWJ, Morris MJ. Time series modelling and interpretation. J R Stat Soc Ser A 1976;139:246–57.
Harrison L, Penny WD, Friston K. Multivariate autoregressive modeling of fMRI time series. Neuroimage 2003;19;1477–91.
Harvey AC. Time Series Models. The MIT Press;1993.
Hesse W, Moller E, Arnold M. Schack B. The use of time-variant EEG Granger causality for inspecting directed interdependencies of neural assemblies. J Neurosci Method 2003;124:27–44.
Hosoya Y. The decomposition and measurement of the interdependency between second-order stationary processes. Probability Theory Relat Fields 1991;88:429–44.
Hosoya Y. Elimination of third-series effect and defining partial measures of causality. J Time Ser 2001;22:537–54.
Kaminski M, Ding M, Truccolo WA, Bressler SL. Evaluating causal relations in neural systems: Granger causality, directed transfer function and statistical assessment of significance. Biol Cybern 2001;85:145–57.
Maravall A, Mathis A. Encompassing univariate models in multivariate time series. J Econometrics 1994;61:197–233.
Pierce DA. R^2 measures for time series. J Am Stat Assoc 1979;74:901–10.
Roebroek A, Formisano E, Goebel R. Mapping directed influence over the brain using Granger causality and fMRI. Neuroimage 2005;25:230–42.
Wiener N. The theory of prediction. In: Beckenbach EF, editors. Modern Mathermatics for Engineers. New York: McGraw-Hill; 1956 (Chapter 8).